2019-2020 Technical Report for SCEC-funded project titled:

Dense, decadal-scale displacement field across the locked-creeping transition zone of the San Andreas fault near Parkfield.

PI: Sean Bemis, Dept. of Geosciences, Virginia Tech

Project Objectives:

Our research spans the transition zone from locked to creeping fault behavior of the San Andreas fault near Parkfield, CA. We have focused on this portion of the fault because most of the San Andreas fault system strain is accommodated within ~1 km of the primary fault trace (e.g., Titus et al., 2006), the 40+ years of intensive research in the Parkfield area, generally sparse vegetation, and the potential to capture complex fault behaviors associated with the transitional nature of the fault behavior. We seek to quantify the cross- and along-fault creep rate changes through the locked-to-creeping transition zone to address the following questions:

- Is there a displacement signal that corresponds with the location of the 2004 Parkfield earthquake?
- Are there detectable zones of localized permanent deformation off the main trace of the SAF?
- What is the shape of the creep rate gradient between the creeping and locked portions of the fault?
- Is the position of the transition zone stable in the position and gradient of the creep rate change?

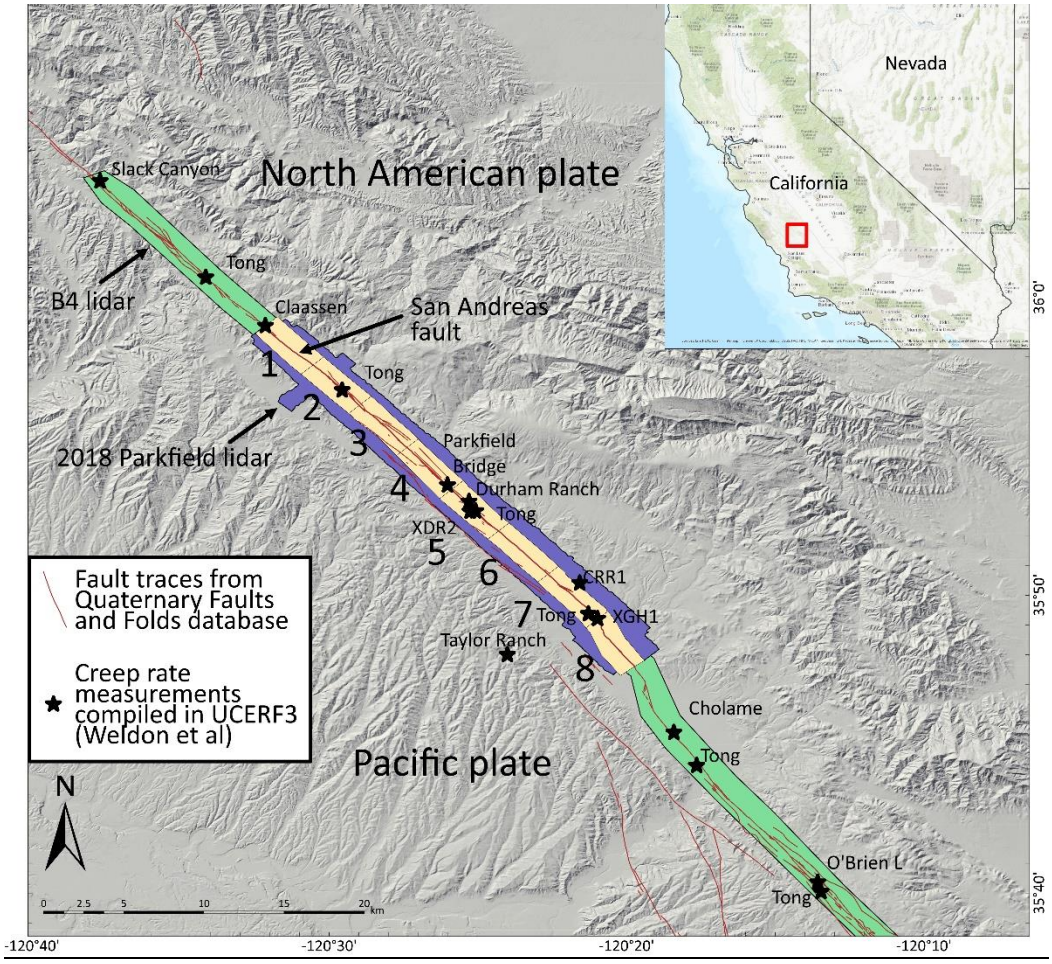

Figure 1. Location map of the central San Andreas fault near Parkfield, showing lidar coverage used in this project (green = B4, purple = 2018 Parkfield), and the area of our measured displacement field (yellow). Black stars show locations of prior creep rate measurements.

Methods:

We use two lidar datasets for our differential topography analyses. The first is data from the B4 Lidar Project, acquired on 05/18/2005 - 05/27/2005 (Bevis and Hudnut, 2005). One stated goal of this dataset is to serve as a baseline for measuring displacements following a future southern San Andreas fault earthquake. The second lidar dataset is the 2018 Parkfield lidar, acquired 05/31/2018 - 06/01/2018 as a NCALM graduate student seed award to Virginia Tech graduate student Michael Vadman (Vadman, 2019). The lidar point cloud densities are 2.98 pts/m^2 and 11.25 pts/m^2, respectively. We use a windowed implementation of the Iterative Closest Point (ICP) algorithm to compute surface displacements between the two datasets. We use a 50 m analysis window slide at 25 m increments on a grid across the datasets.

To filter non-tectonic displacement signals from the data we tested several manual and logical criteria to remove specific signals. The first adjustment we made was to define and apply a global translation to the dataset, because the entire dataset exhibits a northwestward displacement within the time interval, swamping the signal of the relative cross-fault displacement we are seeking as the creep rate. For this,

we selected a patch of the point clouds on the Pacific Plate near the northern end of the swath with minimal noise and a self-consistent displacement signal. We used the average displacement for this patch of the displacement field to normalize the full displacement field. This provides a local North American Plate reference frame to use to calculate cross-fault displacements and changes in the distribution of deformation relative to a fixed point. We also removed displacements within 50 m of the San Andreas fault or an outer boundary of the lidar dataset due to erroneous results from incomplete overlap between the two source lidar datasets and from sampling across the fault. The other non-tectonic signals require more spatially-variable filtering, such as mapping locations of landslides and zones of active erosion. Recognizing limitations on what constitutes realistic creep rate values based on prior measurements and far-field plate motion rates, we applied a series of logical filters based on reasonable limits on tectonic displacement vector magnitude and orientation. These logical filters were tested individually and in combination, with vector magnitude filters removing all values greater than 1 m and 0.5 m, and the orientation filter removing all values outside of 272°-002°, which is a 90° range around the local strike of the San Andreas fault.

To examine the creep rates, we divide the displacement field into a series of along and cross-fault sections, and averaging the displacement vectors within each section. We compare these averages for different approaches to filtering the data, and progressively divide the displacement field into smaller sections.

Results:

The project is still in progress. We report below some of the basic observations around which we build our 2020 SCEC poster.

Our currently level of analysis splits the displacement field into 16 sections – 8 sections along the fault, with each of these being split across the fault. At this scale, each 3.5 km-long section contains thousands of individual displacement measurements. Comparing the number of displacements remaining after the different filter criteria (NA count and PAC count on Table 1) illustrates the degree of scatter in the displacement field because as increasingly restrictive filters are applied, fewer displacement vectors remain. Sections 1-6 only vary by a few degrees and a few mm/yr for the average displacements derived from the different filtered datasets and are broadly consistent with expected/previously-documented creep rates. Conversely, sections 7 and 8 show significant variability in magnitude and orientation between each filter. The contrast between these sections suggests a robust tectonic signal exists in sections 1-6 whereas sections 7-8 is dominated by non-tectonic displacement signals (Table 1). The source of the dominant non-tectonic signal is likely the result of 1) poor ICP fits for the planar agricultural fields, and 2) low creep rates at the southwest end of the transition zone.

Filter	1m, 50m buffer				
Section	Horizontal Displacement (m)	Azimuth	Creep rate (mm/yr)	NA count	PAC count
1	0.281	321	21.6	3353	2864
2	0.257	324	19.8	2805	3449
3	0.163	330	12.5	3673	3072
4	0.06	347	4.6	3409	3146
5	0.117	314	9	3495	3096
6	0.071	317	5.5	3569	2933
7	0.181	121	13.9	3437	3206
8	0.023	70	1.7	3197	2767

Filter	50cm, 50m buffer, 317° ± 45°				
Section	Horizontal Displacement (m)	Azimuth	Creep rate (mm/yr)	NA count	PAC count
1	0.223	314	17.1	1288	1779
2	0.200	318	15.4	1266	2758
3	0.133	317	10.2	2001	2616
4	0.094	316	7.2	1722	1579
5	0.131	309	10	1919	1447
6	0.093	315	7.1	1967	1342
7	0.061	81	4.7	2152	692
8	0.075	315	5.7	1420	909

Filter	1m, 50m buffer, 317° ± 45°				
Section	Horizontal Displacement (m)	Azimuth	Creep rate (mm/yr)	NA count	PAC count
1	0.249	305	19.2	1321	2524
2	0.206	311	15.8	1316	3232
3	0.131	316	10.1	2036	2733
4	0.103	311	7.9	1882	1883
5	0.182	300	14	1978	1978
6	0.134	306	10.3	2032	1749
7	0.032	5	2.5	2210	858
8	0.094	313	7.2	1492	1066

Table 1. Displacement data for 8 along fault sections on both sides of the SAF. Results from 3 different combinations of logical filters are shown, with either 1 m or 50 cm maximum displacement magnitude, a 50 m buffer around the SAF, and an azimuth filter limiting displacements to motion subparallel to the SAF.

Plotting the creep rates for sections 1-6 along the length of the fault illustrates a steep gradient in creep rate, decreasing from ~20 mm/yr to ~6 mm/yr over 5-10 km (Figure 2). This gradient is centered a few kilometers NW of the Parkfield Bridge, whereas a similar steep creep rate gradient defined by prior creep rate measurements (compiled from Weldon et al. (2013)), is roughly centered on the Parkfield Bridge.

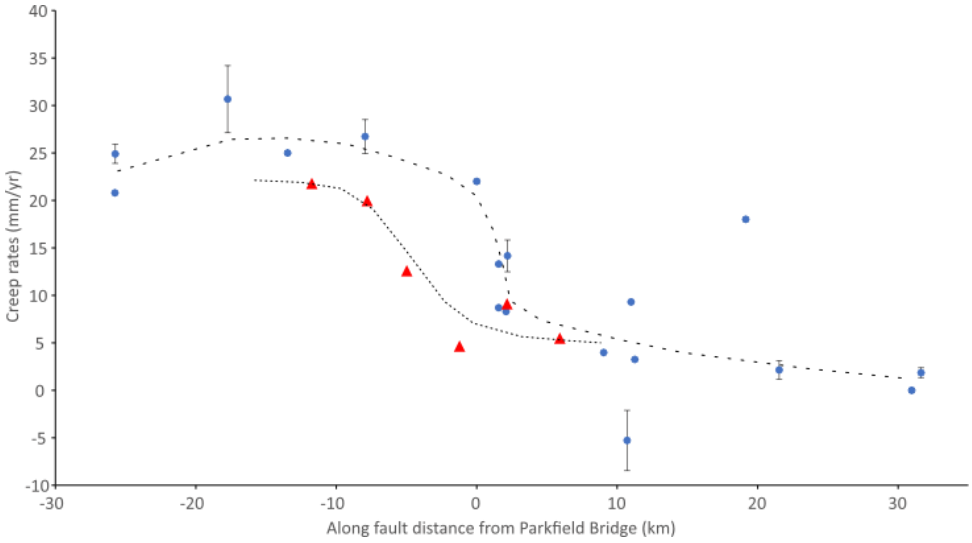

Figure 2. Creep rate measurements along the San Andreas fault near Parkfield. Our preliminary creep rate data (red triangles) are calculated here as the average of the filtered displacement vectors within 3.5 km sections along the fault. Prior creep rate measurements (blue circles) are from the compilation in Weldon et al. (2013)*. The steep gradient in creep rate for the time period of 2005-2018 (our data) appears to have shifted to the NW along the fault by several kilometers relative to the gradient defined by prior creep rate measurements.*

Significance:

The most compelling implication at the current resolution of our analysis is the potential along fault shift in the position of the most rapid transition from creeping to locked (Figure 2). With most of the existing creep rate data on Figure 2 measured prior to the 2004 Parkfield earthquake, and our creep rate data sampling a period that begins ~8 months after this earthquake, it appears that this shift in position is

associated with the 2004 earthquake. We are currently testing this result and developing displacement fields for different periods of time to examine the temporal behavior of this transition zone.

We note here that a recent publication has utilized the same datasets as part of a larger differential topography analysis on the creeping section of the San Andreas fault, and have scooped some of the impact we had hoped for with our analyses. However, our work targets additional behaviors unique to the locked-to-creeping transition zone that we will expand on through continuing this research.

References Cited:

Bevis, M., and Hudnut, K., 2005, Airborne Laser Swath Mapping (ALSM) survey of the San Andreas Fault (SAF) system of central and southern California, including the Banning segment of the SAF and the San Jacinto fault system:

Titus, S.J., DeMets, C., and Tikoff, B., 2006, Thirty-Five-Year Creep Rates for the Creeping Segment of the San Andreas Fault and the Effects of the 2004 Parkfield Earthquake: Constraints from Alignment Arrays, Continuous Global Positioning System, and Creepmeters: Bulletin of the Seismological Society of America, v. 96, p. S250–S268, doi:10.1785/0120050811.

Vadman, M., 2019, Mapping of Displacements near Parkfield, California. National Center for Airborne Laser Mapping (NCALM). Distributed by OpenTopography. https://doi.org/10.5069/G9HD7SRR.

Weldon, R.J., Dawson, T.E., Biasi, G., Madden, C., and Streig, A.R., 2013, Appendix G: Paleoseismic sites recurrence database: US Geol. Surv. Open-File Rept. 2013-1165,.